CONF-851217--52

GRAIN-BOUNDARY, GLASSY-PHASE IDENTIFICATION AND POSSIBLE ARTIFACTS

Y. KOUH SIMPSON*, C. B. CARTER*, P. SKLAD** AND J. BENTLEY**
*Department of Materials Science and Engineering, Cornell University, Ithaca, NY 14853.
**Metals and Ceramics Division, Oak Ridge National Laboratory, Oak Ridge, TN 37831.

CONF-851217--52

DE86 007336

ABSTRACT

Specimen artifacts such as grain boundary grooving, surface damage of the specimen, and Si contamination are shown experimentally to arise from the ion milling used in the preparation of transmission electron microscopy specimens. These artifacts in polycrystalline, ceramic specimens can cause clean grain boundaries to appear to contain a glassy phase when the dark-field diffuse scattering technique, the Fresnel fringe technique, and analytical electron microscopy (energy dispersive spectroscopy) are used to identify glassy phases at a grain boundary. The ambiguity in interpereting each of these techniques due to the ion milling artifacts will be discussed from a theoretical view point and compared to experimental results obtained for alumina.

INTRODUCTION

The presence of an amorphous phase at grain boundaries in ceramic materials can significantly affect their properties. Several transmission electron microscopy(TEM) techniques which can be used to identify such amorphous films at grain boundaries have been reviewed by Clarke[1]; they are the dark-field, diffuse-scattering technique, Fresnel fringe method and high-resolution TEM. In addition, analytical electron microscopy(AEM) using energy dispersive X-ray spectroscopy(EDS) is used to obtain information on the chemistry at grain boundary regions.

During the TEM specimen preparation, however, artifacts such as the Si contamination, surface damage of the specimen and grain-boundary grooving can occur. These artifacts can obscure the experimental results obtained when applying these characterization techniques by giving a misleading impression of the nature of the interface. The experimental evidence for the existence of such artifacts, and their effects on the observations and subsequent interpretations in applying the dark-field, diffuse-scattering technque, Fresnel fringe method and AEM using EDS have been discussed extensively in detail by Kouh Simpson et al [2]. The aim of this paper is to explore further the effects of ion-milling artifacts on the application of these techniques. Specifically, the discussion will be focused on the new, further evidence of the grain boundary grooving in alumina and its implications on the applicability of the dark-field, diffuse-scattering technique and AEM/EDS method.

EXPERIMENTAL

The polycrystalline TEM specimens used in this study were prepared from a commercial alumina(McDanel 998). This material was chosen since it is known to contain a large variety of different types of grain boundaries[3-4]. The TEM specimens were prepared by first cutting the material into 3mm discs and grinding them to a thickness of 50 μms. The subsequent ion-milling was carried out in a commercial ion-miller* with Ar ions at 4 KV until perforation occured. TEM studies were performed with a JEM1200 EX operating at 125 KV.

AEM studies were performed with a Philips EM400T scanning transmission electron microscope (STEM) equipped with a field emission gun (FEG) and EDAX 9100/70 EDS system.

RESULTS AND DISCUSSION

Artifacts Produced From Ion-milling

It is experimentally observed that grooving of grain boundaries[5], locally enhanced Si contamination and structural damage of the surface in polycrystalline aluminas and other materials can occur[2]. Grain boundary grooving is often difficult to detect, since the dimensions of such grooving can be extremely small. Moreover, the grooving characteristics of a grain boundary are intimately related to the character of the grain boundary, the relative orientation of the grain boundary with repect to the specimen surface and grain boundary configuration.

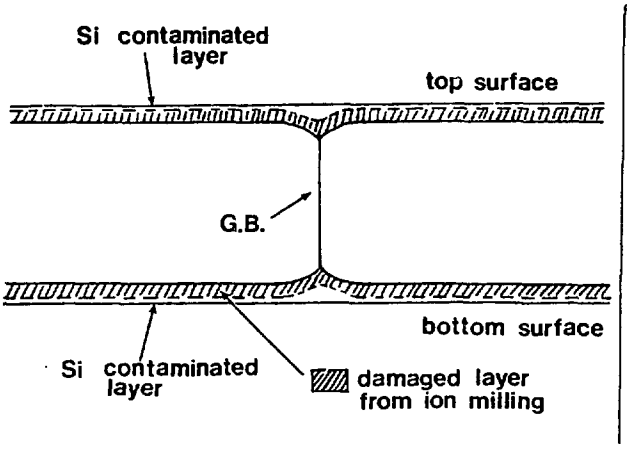

Fig. 1 A schematic diagram of a grooved grain boundary.

Fig. 1 shows a schematic diagram of a grooved grain boundary. There exists a structurally damaged layer on the surface of the specimen produced by the ion beam thinning process. In alumina, Howitt[6] has shown that the damaged layer on the surface produced from ion-milling to be on the order of 10 nm. In addition, the grooves can be filled with amorphous contamination materials which appear to be predominantly Si or C.

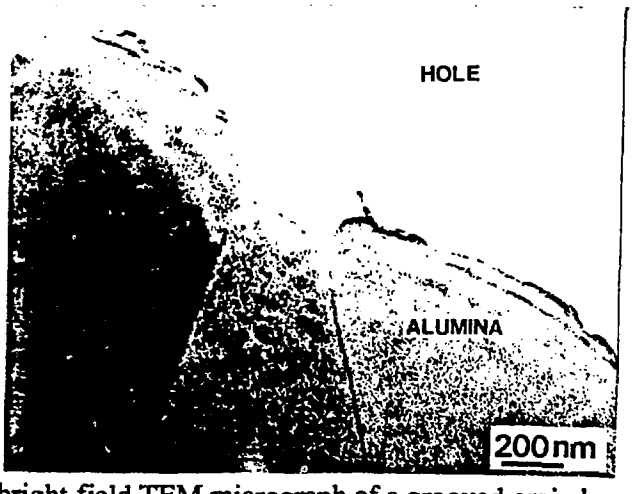

Fig. 2 A bright-field TEM micrograph of a grooved grain boundary in alumina.

The main source for the Si contamination has been found to be the silicone-based, diffusion-pump oil which is used in most commercial ion-millers and carbon evaporators[2]. It has also been found that Si contamination in the electron microscope can occur if beam-sensitive materials that contain Si have been examined recently[7]. Carbon is routinely used to coat non-conductive TEM specimens such as alumina in order to prevent specimen charging. It is proposed in this paper that Ca , along with Si, can also fill these grooves. Fig.2 shows a typical example of grooved grain boundaries in alumina.

The Fresnel-Fringe Method

Figs. 3a, b and c show a high-angle, structured grain boundary in alumina giving rise to the Fresnel-fringe contrast at three different defocus values when the grain boundary is viewed edge-on. However, a periodicity is present in the image when the grain boundary is tilted(Fig. 3d).

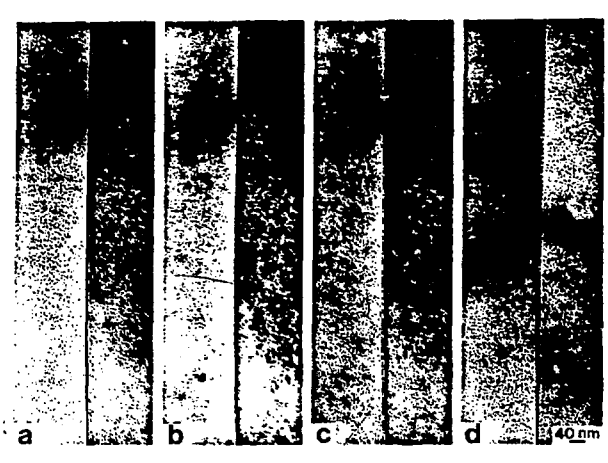

Fig. 3 A high-angle, structured grain boundary in alumina showing Fresnel fringes at the over focused (a), the focused (b), and the underfocused (c) conditions when viewed edge-on. When the grain boundary is tilted (d), however, the interface shows the dislocation contrast.

In general, Fresnel-fringe contrast occurs because as the electron beam passes through an interface region, it experiences a phase shift due to the different mean inner potential present at the interface region in comparison with that of the grains on either side of the boundary. In a structured boundary, the difference in the local mean inner potential occurs because of the lower density at the core of the dislocations present[8]. This mean inner-potential difference will also be influenced by impurity segregation to these cores. If a grain boundary is grooved, amorphous contaminant materials filling these grooves will contribute to the apparent difference in the mean inner potential at the interface with respect to the surrounding grains.

Many reports can be found in literature concerning the Fresnel fringe contrast obtained from various defects. For example, Rühle and Sass [8] reported observations of Fresnel fringes when individual dislocations in NiO grain boundaries were viewed edge-on. A similar effect was observed by Boothroyd and Stobbs [9]for dislocations inclined in the electron beam. Fresnel fringes have been reported for twin boundaries in copper[10] and spinel[11]. The Fresnel fringe contrast can also be observed when there are small cavities present [12]. It can be concluded, hence, that as long as the electron beam experiences a difference in the mean inner potential at the interface, whether it is due to dislocation cores, to compositional differences, or even to local differences in thickness, the Fresnel fringe contrast effect may be seen. It clearly does not, therefore, provide unambiguous evidence for the presence of an amorphous phase.

The Effects Of Grain Boundary Grooving On The Use Of The Dark-field, Diffuse-Scattering And AEM/EDS Techniques

Fig 4a is a dark-field, diffuse-scattering image of a low-angle grain boundary in alumina as viewed edge-on. The grain boundary appears as a bright line in this imaging mode. This result indicates the existence of amorphous materials contributing to the diffuse-scattering in the grain boundary region.

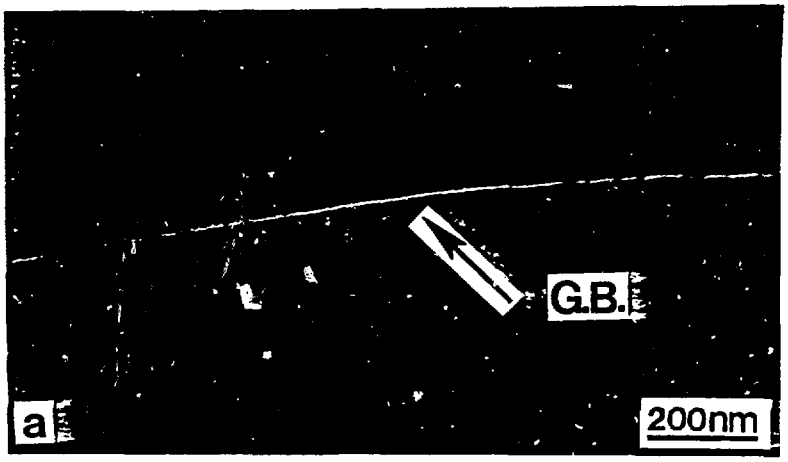

Fig. 4a A dark-field image of a low-angle, structured grain boundary in alumina formed using diffuse scattering(edge-on condition).

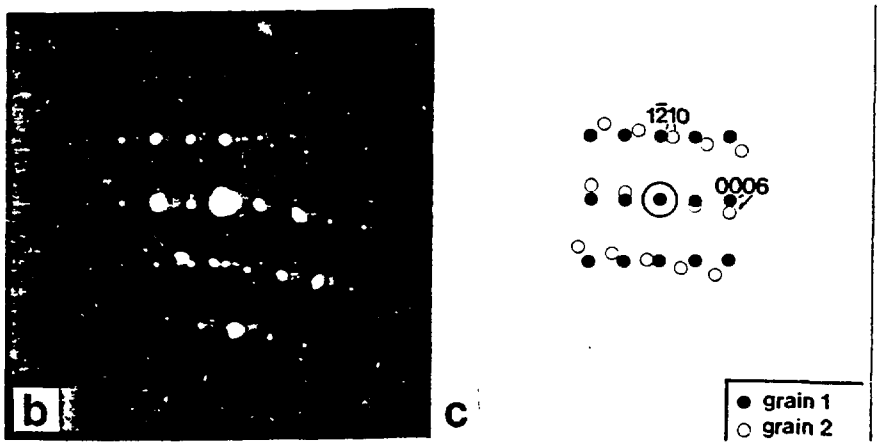

Fig. 4b A selected area diffraction(SAD) pattern obtained from the grain boundary in Fig. 4a.
4c A schematic for the SAD pattern in Fig. 4b. (Tilt angle is ~10 °)

The selected area diffraction(SAD) pattern obtained from this boundary is shown in Fig 4b. As shown in the schematic in Fig. 4c, the tilt angle for this boundary is ~10 °. Assuming that the burger's vector, b, is equal to c(0001) in alumina (1.299nm),and making small angle approximations,the calculated dislocation spacing is 7.46 nm . The measured dislocation spacing is 7.5 nm, which is in excellent agreement with the calculated value. It is , therefore, suggested that this structured low-angle grain boundary is grooved, and that either carbon or some other amorphous contaminant is contributing to the diffuse scattering seen in Fig. 4a. Fig. 4d shows the graph of Si/Al and Ca/Al intensity ratios across this grain boundary in the edge-on condition, indicating the presence of Si and Ca at the grain boundary. The apparent segregation of Si and Ca at grain boundaries in alumina has been reported by other researchers[13-15].

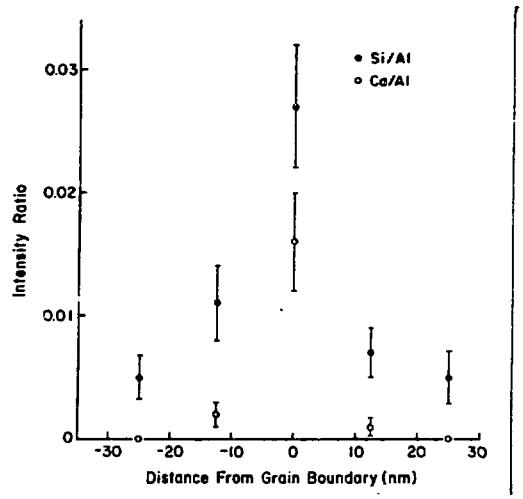

Fig. 4d A graph of Si/Al and Ca/Al X-ray intensity ratios(measured by using STEM/EDS technique and $\lesssim 2$ nm diameter probe) vs. the distace away from the grain boundary in Fig.4a. (profile measured in the edge-on condition).

Figs. 5a and b show the dark-field, diffuse-scattering images of a high-angle grain boundary in an edge-on and a tilted condition respectively. As illustrated in these

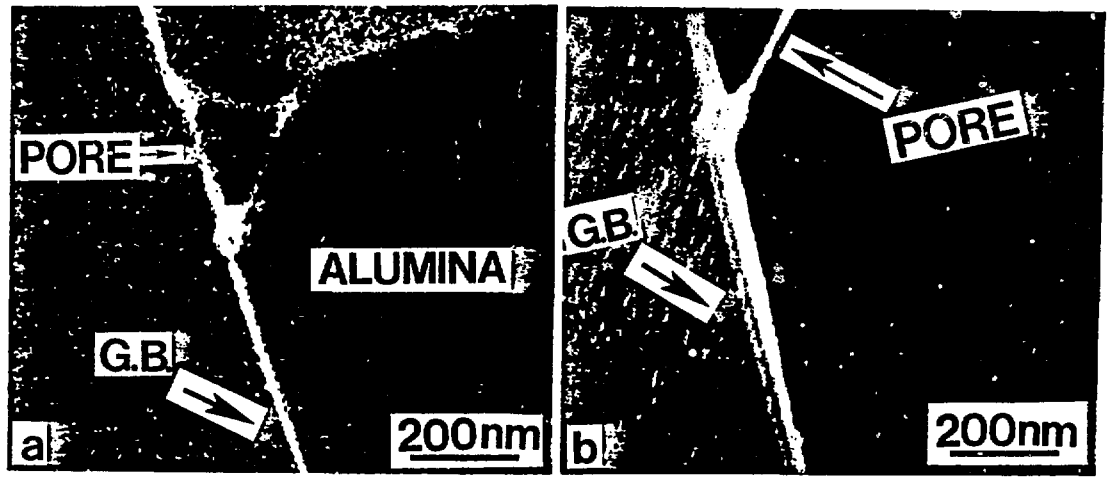

Fig. 5 Dark-field images of a high-angle grain boundary in alumina formed using diffuse-scattering. a)edge-on condition b) the same grain boundary in a tilted condition showing two bright lines with different intensities(displaced aperture).

figures, a grain boundary which appears as a bright line in the edge-on condition may appear as two distinct bright lines at the grain boundary when the grain boundary is tilted. This observation of two bright lines in a tilted condition can be explained by the diagram shown in Fig. 6. When the grooves of a structured grain boundary are filled with any kind of amorphous material, such as Si or C, the grain boundary can light up as two distinct bright lines. However, in this case, the different intensities of the two bright lines may suggest asymetric grooving, as illustrated in Fig. 7. This diagram is similar to that shown in Fig. 6 except that the grain boundary grooving is asymetric for the top and bottom of the specimen.

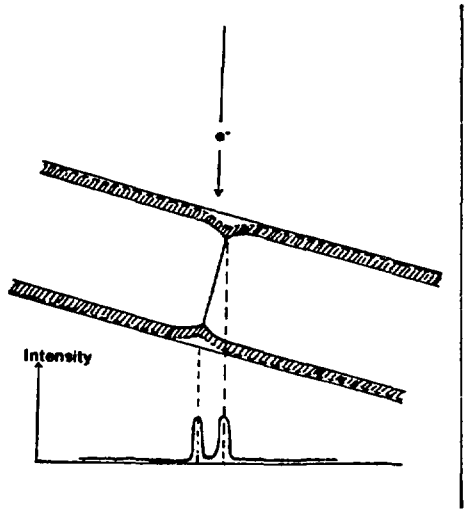

Fig. 6 A schematic diagram of a grooved grain boundary in a tilted geometry. The observation of two bright lines can be due to the amorphous materials filling the grooves at the top and bottom of the specimen at the grain boundary.

Fig. 7 A schematic diagram of a grooved grain boundary with asymetric grooving at the top and bottom of the specimen.

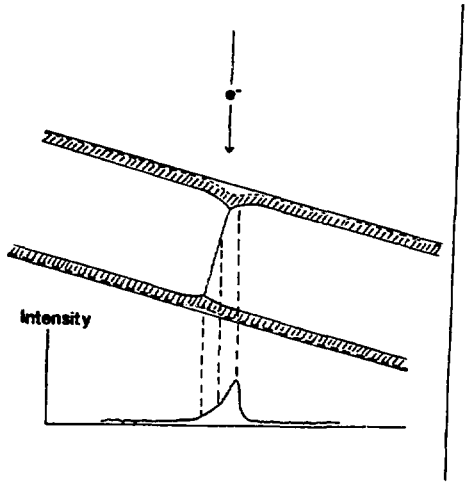

Fig. 8a shows the graph of the profile of Si/Al and Ca/Al X-ray intensity ratios across the grain boundary in Figs. 5a and b in a tilted condition. Both of these ratios monotonically increase within the projected width of the boundary. Fig. 8b shows the graph of the profile of Si/Al and Ca/Al X-ray intensity ratios across the same grain boundary after

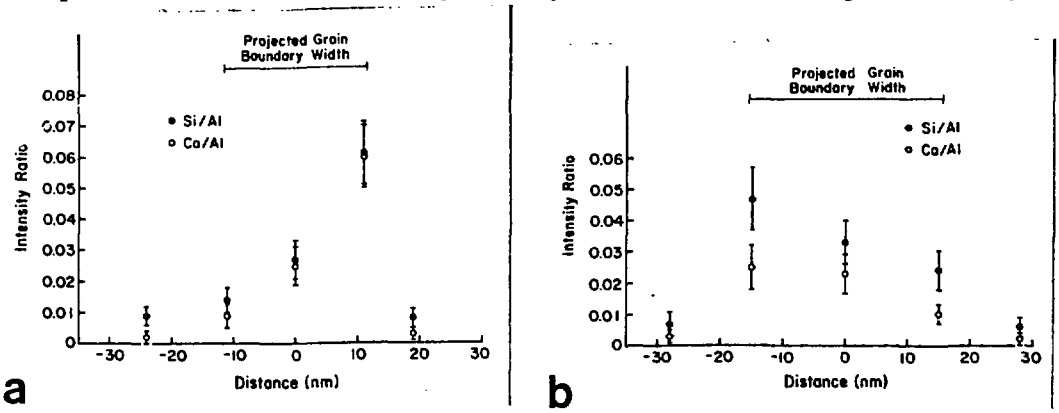

Fig. 8 a) X-ray intensity ratios, Si/Al and Ca/Al, vs. the distance across the grain boundary when the boundary is viewed in a tilted geometry with respect to the electron beam. b) the same set of X-ray intensity ratios taken after the specimen has been inverted in the manner described in Fig. 9.

the specimen has been inverted in the manner as illustrated in Fig. 9. After inverting the specimen, both the Si/Al and Ca/Al ratios show a monotonic decrease away from the maximum value. Since beam broadening and absorption effects are calculated to be negligible in this case, this result indicates that regardless of being on the top or at the bottom of the specimen with respect to the impinging electron beam, one side of the specimen consistently shows higher concentration in both Si and Ca.

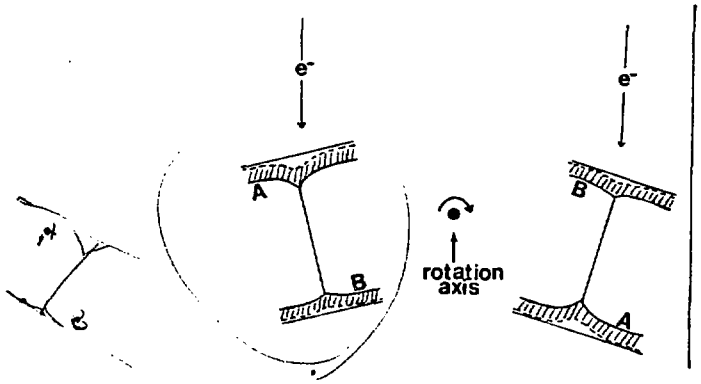

Fig. 9 A diagram showing the manner in which the specimen has been inverted before collecting the X-ray information shown in the graph in Fig. 8b.

The above result can be again explained, for example, by the asymetric grooving at the boundary as illustrated in Fig.7. Without the presence of these grooves, and neglecting beam broadening and any absorption effects, as is the case in this experiment, no large variation in the Si and Ca concentrations across the grain boundary is to be expected in a tilted condition . Also, the fact that Ca/Al ratio varies in the same manner as the Si/Al ratio suggests the preferential accumulation of Ca along with Si in the grooves. One source for this Ca contamination may be the numerous glassy pockets that are present at the triple points in many commercial aluminas such as the type examined in this study. These glassy(or possibly crystalline) pockets can be sputtered during ion-milling, filling the grain boundary grooves with Ca and Si that are normally present at these triple point pockets. As shown in Fig. 5a and b, this grain boundary is connected to a pore at the triple point which may have been sputtered during ion-milling. Ca concentration inside the grain away from the grain boundary is found to be approximately at the level near the detectability limit of AEM/EDS technique. Ca segregation on the free surface of single crystal alumina has been shown by Baik et al [16] using Auger technique. In this study, the thickness of the Ca segregation layer at the surface of alumina has been shown to be up to 1 monolayer[17].

Fig.10 is a profile across the grain boundary in Figs. 5a and b when the boundary is viewed edge-on. The Si/Al and Ca/Al X-ray intensity ratios at the grain boundary are both higher than those at the grain boundary when the boundary is tilted as in Graphs shown in Figs. 8a and b. This result is consistent with the fact that the value at the grain boundary should be the highest when it is edge-on, since the entire grain boundary column is then within the impinging electron beam.

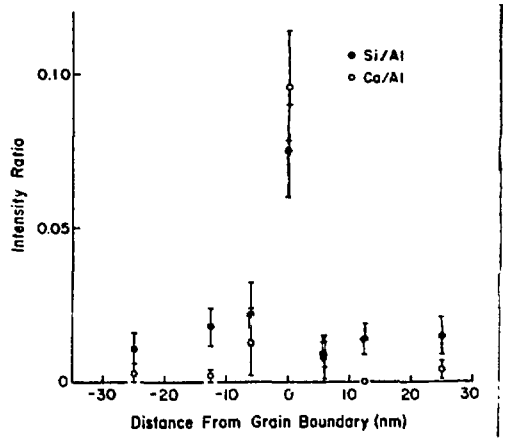

Fig. 10 X-ray intensity ratios, Si/Al and Ca/Al, vs. the distance across the grain boundary of Figs. 5a and b when viewed edge-on.

CONCLUSIONS

During the TEM specimen preparation, particularly the ion-milling and carbon-coating processes, Si and Ca contamination, surface damage of the specimen and grain boundary grooving can arise. These specimen artifacts can give misleading impressions concerning the nature of the grain boundaries since they can appear to suggest the presence of a glassy phase. Particularly, in the case of the dark-field, diffuse-scattering technique and the Fresnel-fringe method, grain boundary grooving can give ambiguous results as to the actual nature of the internal interface. The concentration profiles obtained by tilting a grain boundary using AEM/EDS technique give further evidence that the grain boundary grooving occurs.

ACKNOWLEDGEMENTS

The authors would like to thank Mr. Ray Coles for maintaining the microscopes at Cornell. This research is supported by the U.S. Department of Energy under grant number DE-FG02-84ER45092 at Cornell, and by the Division of Materials Sciences, U.S. Department of Energy under contract number DE-AC05-84OR21400 with Martin Marietta Energy Systems, Inc., and under contract number DE-AC05-76OR00033 with Oak Ridge Associated Universities (SHaRE program).

*The ion-miller is manufactured by Techniques and contains a silicone-based diffusion pump oil.

REFERENCES

1. D. R. Clarke, Ultramicroscopy, 4, 33 (1979).
2. Y. Kouh Simpson, C. B. Carter, K.J. Morrissey, P. Angelini and J. Bentley, J. Mat. Sci., In Press (1985).
3. K. J. Morrissey and C. B. Carter, J. Am. Ceram. Soc., 67, (4), 292 (1984).
4. C. B. Carter and K. J. Morrissey, Advances in Ceramics, 10, 303,(1984).
5. M. Ruhle, private communication (1985).
6. D. G. Howitt, J. Elect. Mic. Tech., 1, (4), 405 (1984).
7. J. T. Schwartz, private communication (1985).
8. M. Rühle and S. L. Sass, Phil. Mag. A., 49, (6), 759(1984).
9. C. B. Boothroyd and W. M. Stobbs, Phil. Mag. A., 49,(1), L5-L8 (1984).
10. W. M. Stobbs and D. J. Smith, Inst. Phys. Conf. Ser. 61, 373(1981).
11 Z. Elgat, PhD Thesis, Cornell Univ., Ithaca, NY (1985).
12. S. Iijima, Optik, 47(4), 437 (1977).
13. W. C. Johnson, D. F. Stein and R. W. Rice, 4th Bolton Landing Conf., 261(1974).
14. W. C. Johnson and R. L. Coble, J. Am. Ceram. Soc., 61(3-4), 110(1978).
15. W. D. Kingery, Pure & Appl. Chem., 56(12), 1703-1714(1984).
16. S. Baik, D. E. Fowler, J. M. Blakely and R. Raj, J. Am. Ceram. Soc., 68,(5), 281(1985).
17. S. Mitra, private communication (1985).